Screening Anti-Cancer Drugs against Tubulin using Catch-and-Release Electrospray Ionization Mass Spectrometry

Reza Rezaei Darestani[1], Philip Winter[2], Elena N. Kitova[1], Jack A. Tuszynski[2] and John S. Klassen[1]*

[1]*Department of Chemistry and Alberta Glycomics Centre, University of Alberta, Edmonton, Alberta, Canada T6G 2G2*

[2]*Department of Oncology, University of Alberta, Edmonton, AB, Canada T6G 1Z2*

* Email: john.klassen@ualberta.ca

Abstract

Tubulin, which is the building block of microtubules, plays an important role in cell division. This critical role makes tubulin an attractive target for the development of chemotherapeutic drugs to treat cancer. Currently, there is no general binding assay for tubulin-drug interactions. The present work describes the application of the catch-and-release electrospray ionization mass spectrometry (CaR-ESI-MS) assay to investigate the binding of colchicinoid drugs to αβ-tubulin dimers extracted from porcine brain. Proof-of-concept experiments using positive (ligands with known affinities) and negative (non-binders) controls were performed to establish the reliability of the assay. The assay was then used to screen a library of seven colchicinoid analogues to test their binding to tubulin and to rank their affinities.

Introduction

The αβ-tubulin heterodimers are the building blocks of microtubules (MTs) [1], which are long, hollow, cylindrical protein polymers and dynamic structural components of the eukaryotic cytoskeleton [2-5]. Both the α and β subunits exist as different isotypes in many organisms, with dissimilar relative amounts, e.g. there are six main isoforms of both α (αI-VI) and β (βI-VI) subunits in mammals, differing from each other in their amino acid sequences and encoded by different genes [6,7]. Microtubules control cell shape and play important roles in mitosis, intracellular vesicle transport, organization, and positioning of membranous organelles [8-10]. The critical role of microtubules in cell division makes them an attractive target in cancer chemotherapy. Microtubule targeting agents (MTAs) modify the formation and function of MTs by altering microtubule dynamics [11]. These MTAs interact with tubulin so as to stabilize or destabilize the polymeric microtubules, in each case leading to cell cycle arrest. In general, drugs that interact with microtubules are divided in two groups: (i) microtubule stabilizers, which include taxanes [12], epothilones [13], discodermolide [14], and peloruside A [15], and (ii) microtubules destabilizers, including colchicinoids [16], vinca alkaloids [17], dolastatin [18], and hemiasterlins [19].

Of the known MTAs, taxol, colchicine, and vinblastine are among the best characterized and most widely used clinically [20]. Colchicine binds at the interface of the α and β subunits [21], while taxol and vinblastine bind to β subunit but in different domains. Colchicine has been widely used to treat gout, familial Mediterrenian fever and auto-inflammatory diseases [22,23]. It is an alkaloid found in *Colchium autmnale* and *Gloriosa superba* and is composed of three rings, a trimethoxy benzene ring (ring A), a methoxy tropone ring (ring C), and a seven-membered ring (ring B) [16]. The administration of colchicine inhibits the cell division process through two proposed mechanisms. In the first mechanism, referred to as the end-poisoning mechanism, polymerization is inhibited through colchicine binding to the ends of the microtubules, thus preventing the microtubules growth by sterically blocking further addition of the tubulin dimers. The other mechanism focuses on colchicine binding-induced conformational changes in the tubulin dimers, which leads to the inhibition of microtubule assembly or disassembly of the microtubules [9,16,24]. However, the high concentrations of colchicine required to effectively kill cancer cells also adversely affects non-tumoral cells leading to significant dose-limiting side effects. Consequently, extensive research to design analogues of colchicine (e.g. combretastatin A4) [25] or colchicine derivatives with improved binding (to MTs), thereby lowering the required therapeutic does and widening the therapeutic window, has been underway in recent years [26].

As reported originally by Diaz and co-workers [16,27,28], the association of colchicine to tubulin appears to be a two-step process – a fast, reversible step, followed by a slow, reversible step, eq 1:

$$T + C \underset{}{\overset{K_1}{\rightleftharpoons}} TC \underset{k_{-2}}{\overset{k_2}{\rightleftharpoons}} TC' \qquad (1)$$

where T, C, TC and TC' represent tubulin dimer, colchicine, and the non-covalent tubulin-colchicine complexes, respectively, and K_1 is the equilibrium constant of the fast reversible step and k_2 and k_{-2} are the rate constants for the forward and reverse reactions of the second step. It was originally proposed that colchicine binds to the αβ-tubulin dimer initially through a single ring (ring C), corresponding to the fast step [29,30], followed by conformational changes in tubulin associated with insertion of ring A and B to give a higher affinity interaction [29,30].

However, it was later suggested by Banerjee and *et al.* that the biphasic nature of the colchicine-tubulin binding kinetics is related to the differential binding of colchicine to the β-tubulin isotypes [16,31]. For example, different k_2 values were measured for the four β-isotypes found in bovine brain as 132 ± 5 M^{-1} s^{-1} (αβII), 30 ± 2 M^{-1} s^{-1} (αβIII), and 236 ± 7 M^{-1} s^{-1} (αβI and αβIV) [31].

Currently, no general binding assay exists for tubulin interactions with colchicinoid drugs, as well as other classes of MTAs. The use of isothermal titration calorimetry (ITC), which represents the gold standard for quantifying protein-ligand interactions *in vitro*, is limited by the relatively long equilibration times required for these interactions (Figure S1, Supplementary Information). Radiolabeling assays have previously been used to study tubulin-colchicine binding. However, the radiolabeled compounds are expensive and require special handling, disposal and detection. Fluorescence assays have also been used to quantify colchicine binding to tubulin [9,32]. The main advantage of these methods is that neither requires the labeling of drugs nor the separation of free colchicine from the complex [9]. However, some colchicine analogues (e.g. thiocolchicine) exhibit little or no fluorescence in such assays and cannot be studied using this approach [9,33]. Therefore, there is a significant need for a general and robust assay to measure the affinities of colchicine analogues for tubulin. This would enable a reliable characterization and ranking of novel tubulin-binding ligands with greater specificity and selectivity for the targets, which could exhibit subtle but important structural differences such as found in tubulin isotypes and mutants.

Recently, the direct electrospray ionization mass spectrometry (ESI-MS) assay has emerged as a powerful tool for measuring the affinities of protein-ligand interactions *in vitro* [34-39]. The assay is based on direct measurement of the relative abundances of the ligand-bound and free protein ions measured by ESI-MS. This assay has a number of strengths that make it a valuable technique for binding measurements including simplicity (no labeling or immobilization is required), speed (measurements can be completed within a few minutes) and low sample consumption (typically <pmol per analysis). The ability to measure multiple binding equilibria simultaneously makes the ESI-MS assay well suited for screening libraries of compounds against target proteins [38,39]. Where direct detection of the protein-ligand complexes by ESI-MS is not possible, due to factors such as high molecular weight (MW) or protein heterogeneity, the catch-and-release (CaR) ESI-MS assay can be employed [40-47]. In this assay, ligand binding is established by releasing (as ions) ligands bound to the protein in the gas phase using activation methods such as collision-induced dissociation (CID). Typically, ligands can be identified based on their measured MW; in some cases fragmentation of the released corresponding ligand ion or ion mobility separation (IMS) may be required for positive identification. The CaR-ESI-MS assay has been used to screen carbohydrate, peptide and small molecule libraries against target proteins [40-47]. However, the reliability of the method has only been rigorously tested in the case of carbohydrate libraries [40,41,45-47].

Here, we describe the application of the CaR-ESI-MS assay to investigate the binding of several colchicinoid drugs to αβ-tubulin dimers extracted from porcine brain. First, proof-of-concept experiments, using positive (ligands with known affinities) and negative (non-binders) controls, were performed to establish the reliability of the assay for detecting tubulin-colchicinoid drugs interactions. The assay was then used to screen a small library of seven colchicinoid analogues to test their binding to tubulin and to rank their affinities.

Experimental

Proteins

αβ-tubulin dimer (MW ~110 kDa), extracted from porcine brain, was purchased from Cytoskeleton, Inc. (Denver, CO). Bovine Serum Albumin (BSA) was purchased from Sigma-Aldrich Canada (Oakville, Canada). A stock solution of αβ-tubulin dimer was prepared by dissolving a known mass of protein in 500 μL of aqueous ammonium acetate (50 mM, pH 6.8, at 4 °C) and concentrated to 5 mg mL^{-1} (~40 μM) by ultracentrifugation using a Vivaspin a 0.5 mL centrifugal filter (Sartorius Stedim Biotech, Göttingen, Germany) with MW cutoff of 30 kDa. The stock solution was then separated into aliquots, which were snap frozen in liquid nitrogen and then stored at -80 °C until needed. The stock solution of BSA was prepared by dissolving a known mass of protein in deionized water, followed by buffer exchange into ammonium acetate (50 mM, pH 6.8) using a Vivaspin 0.5 mL centrifugal filter (Sartorius Stedim Biotech, Göttingen, Germany) with MW cutoff of 10 kDa. The stock solution, with a final concentration of 500 μM, was then stored at 4 °C.

Drugs

Colchicine (**L1**, MW 399.2 Da) and thiocolchicoside (**L8**, MW 563.6 Da) were purchased from Sigma-Aldrich Canada (Oakville, ON) and Abcam Inc. (Cambridge, UK), respectively. Vincristine sulfate (**L9**, MW 824.4 Da) was purchased from Sigma-Aldrich Canada (Oakville, ON). The colchicine analogues (**L2**, MW 415.1 Da; **L3**, MW 445.2 Da; **L4**, MW 510.2 Da; **L5**, MW 526.1 Da; **L6**, MW 554.2 Da; **L7**, MW 587.2 Da) were synthesized by ChemRoutes Corp. (Edmonton, Canada). The structures of **L1** – **L8** are given in Figure 1a and **L9** in Figure 1b. The purity of all ligands was determined to be >95% by liquid chromatography (LC)-MS (Agilent Eclipse plus C18 column, 250 mm × 4.6 mm, 5 μm particle size; mobile phase, water/acetonitrile (0.1% HCOOH) 80:20 to 5:95 over 5 min and held for 1.5 min; flow rate 0.5 mL/min). Stock solutions of 20 mM of each of **L1** – **L8** were prepared by dissolving a known mass of compound into DMSO and then diluting with deionized water and stored at -20 °C.

Mass spectrometry

All of the ESI-MS measurements were carried out in positive ion mode using a Waters Synapt G2S quadrupole-ion mobility separation-time of flight (Q-IMS-TOF) mass spectrometer (Manchester, UK) equipped with a nanoflow (nanoESI) source. A P-1000 micropipette puller was used to produce nanoESI tips from borosilicate capillaries (1.0 mm o.d., 0.68 mm i.d.) (Sutter Instuments, Novato, CA). A voltage of ~1.3 kV was applied to platinum wire inserted into the nanoESI tip to carry out ESI. A source temperature of 60 °C and cone voltage 10 V were used for all measurements. Data acquisitions and processing were performed using MassLynx software (version 4.1).

CaR-ESI-MS Assay

To carry out CaR-ESI-MS, the quadrupole mass filter was set to pass ions with a range of *m/z* values (4000 – 7000), unless otherwise noted. The quadrupole parameters were set to: mass 1, 2, and 3 at 3000, 4000, and 5000 *m/z*, respectively, with dwell times of 5% for mass 1 and 2, ramp time for *m/z* 3000 at 5% and for *m/z* 4000 at 85%. Selected ions were then subjected to CID in the Trap region using collision energies ranging from 2 to 140 V and the released ligand ions identified based on the measured *m/z*. Where indicated, and following CID in the Trap region, the tubulin ions were subjected to another stage of CID in the Transfer region, using collision energies ranging from 1 to 120 V. Prior to the second stage of CID, the tubulin ions were separated from free ligand ions using IMS. For IMS, a wave height of 40 V and a wave velocity between 400 and 700 m s^{-1} were applied; helium and nitrogen (IMS gas) gas flow rates were 80 and 70 mL min^{-1}, respectively. In all cases, data acquisition and processing were performed using MassLynx software ver. 4.1 (Waters, Manchester, UK).

Result and Discussion

Analysis of tubulin-colchicine binding by ESI-MS

As a starting point for this study, ESI-MS was used to analyze aqueous solutions of tubulin, on its own and in the presence of **L1** (colchicine). Shown in Figure 2a is a representative ESI mass spectrum acquired for an aqueous ammonium acetate solution (100 mM, pH 6.8) of αβ-tubulin (14 μM). Abundant ion signal corresponding to tubulin dimer (d^{n+}), at charge states +18 - +22, is evident; low abundance signal corresponding to tubulin tetramer ions, at charge states +32 - +29, was also detected. The measured MWs of dimer (101,750 ± 12 Da) and tetramer (203,460 ± 52 Da) from porcine brain (mostly αI and βI) [48,49] are in agreement with theoretical values (UniProt, P02550 for αI and P02554 for βI) of 101,677 Da and 203,354 Da, respectively. The presence of tetramer could be due to self-association of the tubulin dimer; nonspecific binding during the ESI process might also play a role in its formation [38,39]. Because the stock solutions of **L1** – **L8** contained DMSO, ESI mass spectra were also acquired for aqueous solutions of tubulin in the presence of low concentrations of DMSO. Shown in Figure 2b is a representative ESI mass spectrum obtained under the same conditions as those used for Figure 2a, but with the presence of 0.05% v/v DMSO. This percentage of DMSO corresponds to amount used in all of the binding measurements carried out in the present study, *vide infra*. It can be seen that, at this concentration, DMSO has little effect on the appearance of the mass spectrum, although there is a slight shift in the charge state distribution, to lower values (+17 to +21), of the tubulin dimer. However, it should be noted that charge state distribution measured for the tubulin dimer ions may vary slightly between mass spectra, *vide infra*.

Shown in Figures 2c-f are the ESI mass spectra of aqueous ammonium acetate buffer (100 mM) solutions of αβ-tubulin (14 μM) and a range of colchicine (**L1**) concentrations (2-20 μM) following incubation at 37 °C for 1 h. While it was not possible to directly ascertain the presence of ions corresponding to **L1**-bound tubulin dimer from the mass spectra, the presence of **L1** in solution resulted in a small but measurable increase in the *m/z* of the tubulin dimer ions and the magnitude of the effect increased with increasing **L1** concentration. This observation is consistent with the presence of **L1**-bound tubulin dimer in solution. (Figure S2, Supplementary Information)

To conclusively establish the presence of tubulin-bound **L1**, the CaR-ESI-MS assay was employed. As a starting point, the quadrupole mass filter was set to pass all ions, with *m/z* between 4000 and 7000, produced from a solution of αβ-tubulin (14 μM); these were then subjected to CID in Trap region using collision energies ranging from 2 to 140 V (Figure S3a, Supplementary Information). It can be seen that the tubulin ions are stable and do not undergo any fragmentation, even at highest collision energies. In the same way, the Car-ESI-MS assay was applied to tubulin ions produced from a solution of αβ-tubulin (14 μM) and **L1** (14 μM) (Figures S3b, Supplementary Information). It can be seen that CID resulted in the appearance of signal corresponding to protonated **L1** (*m/z* 400.1) at all of the energies investigated. These results confirm that **L1** was bound to the gaseous tubulin ions.

In order to rule out the possibility that the **L1**-tubulin interactions identified by CaR-ESI-MS arose during the ESI process (i.e., due to nonspecific binding), the measurements were repeated using a solution of αβ-tubulin (14 μM), **L1** (14 μM) and BSA (14 μM) (Figure S4, Supplementary Information). To the best of our knowledge BSA does not interact with **L1** in solution and, therefore, served as a reference protein (P_{ref}) to test for nonspecific binding.

Isolation of the +18 charge state of the tubulin dimer, followed by CID resulted in the appearance of protonated **L1** (Figure S4, Supplementary Information). In contrast, isolation of the +16 charge state of BSA, followed by CID failed to produce any signal corresponding to **L1** (Figure S4, Supplementary Information). Taken together, these results suggest that the gaseous **L1**-bound tubulin ions are the result of specific binding in solution, with little or no contribution from non-specific binding during the ESI process.

As described above, **L1** binding to tubulin dimer is accompanied by a change in conformation. Therefore, it was of interest to investigate whether the binding of **L1** to tubulin could be quantified based on differences in the collision cross sections of the free and ligand-bound tubulin dimer ions. To assess whether the ligand binding-induced conformational changes result in measurable differences in collision cross sections, IMS arrival time distributions (ATDs) were measured for tubulin dimer ions produced from solutions containing αβ-tubulin alone (14 μM) and in the presence of **L1** in ammonium acetate solution (100 mM, pH 6.8) (Figure S5, Supplementary Information). Inspection of the ATDs measured for each charge state reveals no measurable differences for tubulin dimers produced in the absence or presence of **L1**, even at the highest concentration (28 μM) of **L1** investigated.

Taken together, the aforementioned results reveal that, with the current instrumentation, it is not possible to directly quantify tubulin- **L1** interactions using ESI-MS. Consequently; subsequent efforts were directed towards the possibility of ranking ligand (drug) affinities for tubulin using CaR-ESI-MS. As a starting point, a series of control experiments were carried out to assess the reliability of the approach and to identify optimal instrumental conditions for its implementation. Important requirements when using CaR-ESI-MS to rank affinities based on the relative abundances of the released ligand ions are that the release and ionization efficiencies be similar for all of the bound ligands. Because of differences in the nature of the intermolecular interactions for different ligands in the gaseous protein-ligand complex ions, the dissociation (release) rate constants are expected to vary, possibly significantly, between ligands. Consequently, the condition of uniform release efficiencies can only reliably be achieved by fully releasing all bound ligands (i.e., complete dissociation). Based on the changes in the abundance of **L1** relative to the d^{+18} - d^{+21} ions, with collision energy (in the Trap region) measured in the mass spectra shown in Figure S6 (Supplementary Information), complete release appears to be achieved at energies ≥100 V. To further support this conclusion, the tubulin ions were subjected to a second stage of CID in the Transfer region. Shown in Figures S7a and S7b (Supplementary Information) are CID mass spectra acquired at Trap and Transfer voltages of 100 V and 1 V, respectively (Figure S7a, Supplementary Information), and 1V and 100 V, respectively (Figure S7b, Supplementary Information). In both cases, abundant protonated **L1** is detected. Shown in Figures S7c and S7d (Supplementary Information) are CID mass spectra acquired using Trap and Transfer voltages of 100 V and 1 V, respectively (Figures S7c, Supplementary Information) and 100, V and 100 V, respectively, (Figures S7d, Supplementary Information). These data were acquired using IMS to exclude (based on arrival times) the contribution of any **L1** ions released in the Trap region from the CID mass spectra. It can be seen that, in both cases, no measurable signal corresponding to **L1** ions, resulting from ligand release in the Transfer region, was detected. These results confirm that **L1** is fully released from the tubulin ions at Trap voltages ≥100 V.

To further validate the CaR-ESI-MS assay, it was applied to a solution of a αβ-tubulin (14 μM), **L1** (14 μM) and vincristine (**L9**, 14 μM). These ligands have different binding sites on tubulin and slightly different affinities. As discussed above, the affinity of **L1** for tubulin dimer is reported to be in the 0.5×10^6 to 3×10^6 M^{-1} range, while for **L9** the affinity is slightly lower, 0.1×10^6 to 0.5×10^6 M^{-1} [5,32]. Shown in Figure 3a is a representative ESI mass spectrum acquired for a solution of tubulin (14 μM) with **L1** (14 μM) and **L9** (14 μM); shown in Figures 3b-f are CID mass spectra measured in the Trap region at collision energies ranging from 25 to 120 V. Signals corresponding to both protonated **L1** (*m/z* 400.1) and **L9** (*m/z* 825.4) are evident in the CID spectra and the **L1** to **L9** abundance ratios reach a constant value at Trap voltages ≥80 (Figure 4a). Notably, the measured **L1** to **L9** abundance ratios measured at these higher collision energies are in good agreement with the expected ratio calculated from the reported affinities (Figure 4b). Similar results were obtained at the two other ligand concentrations tested (Figure 4b). These results suggest that **L1** to **L9** exhibit similar release and ionization efficiencies.

Analogous measurements were carried out on solutions of αβ-tubulin (14 μM), **L1** (14 μM), vincristine (**L9**) (14 μM) and thiocolchicoside (**L8**) (14 μM). **L8** does not bind to tubulin and served as a negative control. Shown in Figure S8a (Supplementary Information) is a representative ESI mass spectrum; the corresponding CID spectrum measured at a Trap voltage of 120 V is shown in Figure S8b (Supplementary Information). It can be seen that both protonated **L1** and **L9** are released from tubulin. However, signal corresponding to **L8** was not detected at any of the collision energies investigated. Measurements carried out at different concentrations of **L1**, **L8** and **L9** produced similar results (data not shown). The results of these control experiments suggest that the CaR-ESI-MS assay can be used to detect ligand binding to tubulin in solution and, by screening libraries of compounds, to rank their affinities.

Library screening

Having established the reliability of the CaR-ESI-MS assay for detecting tubulin-drug interactions *in vitro*, the assay was used to screen a small library of colchicinoids (**L1–L7**) against tubulin to identify the strongest binder. Shown in Figure 5 are the representative CID mass spectra acquired for an aqueous ammonium acetate (100 mM, pH 6.8) solution of αβ-tubulin (14 μM) incubated with the library (**L1–L7**, 2 μM each) at 37 °C for 1 h. Inspection of the mass spectra reveals evidence for the release of all seven ligands as singly protonated ions, **L1** (400.1 *m/z*), **L2** (416.1 *m/z*), **L3** (446.1 *m/z*), **L4** (511.1 *m/z*), **L5** (527.1 *m/z*), **L6** (555.5 *m/z*), **L7** (588.5 *m/z*). The relative abundance of each ligand was measured as a function of Trap voltage. Similar to what was found for the abundances of released **L1** and **L9** (Figure 4), a constant abundance ratio was measured at voltages ≥100V (Figure 6a). The relative abundances of the released ligand ions, measured at these higher energies, suggest the following trend in affinities: **L3** > **L2** ~ **L1** ~ **L5** > **L4** > **L6** ~ **L7** (Figure 6b). Analogous measurements were repeated at different concentrations of ligands (**L1 – L7,** 2 and 7 μM total concentration) under the same conditions. Notably, the same trend in affinities was observed at all of the concentrations investigated. On their own, the CaR-ESI-MS screening results suggest that the colchicinoid **L3** may be a more potent MTA than **L1**. Biological activity studies will now be carried out to validate this finding.

Conclusions

Taken together, the results of this study suggest that the CaR-ESI-MS assay could aid in detecting specific drug interactions with tubulin dimers *in vitro* and, when applied to libraries, to rank their affinities. To our knowledge, this is the first reported example of the application of the CaR-ESI-MS assay in the area of anti-cancer drug screening. Proof-of-concept experiments carried out on αβ-tubulin dimers extracted from porcine brain using positive (known ligands) and negative (non-binders) controls were performed to establish the reliability of the assay. The assay was then used to screen a library of seven colchicinoid analogues to test their binding to tubulin and to rank their affinities. The ultimate utility of this methodology lies in applying it as a means of selecting compounds that target specific isotypes of tubulin or specific mutants of tubulin. The reason for this is that tubulin is an abundant protein common to all cells in the body. However, the distribution of tubulin isotypes is different for all cell types and especially for cancer cells [50]. Therefore, the idea of targeting an isotype of tubulin that is highly expressed in cancer cells and much less so in normal cells would lead to an optimization of treatment efficacy and minimization of side effects [51]. A computational algorithm for such a selection process from a library of tubulin-binding ligands has recently been published [52]. What is missing, however, is an experimental methodology whereby compounds can be ranked according to their affinity for tubulin isotypes, which would validate computational predictions. The present paper is intended to demonstrate that such a method is now emerging and, with future refinement, can be developed into a powerful platform for the drug discovery process.

Acknowledgement

The authors are grateful for financial support provided by the Natural Sciences and Engineering Research Council of Canada and the Alberta Glycomics Centre.

References

1. Nogales, E., Wolf, S. G., Dowling, K. H.: Structure of the alpha beta tubulin dimer by electro crystallography. Nature **391,** 199-203 (1998).
2. Bryan, J., Wilson, L.: Are Cytoplasmic Microtubules Heteropolymers? Proc. Natl. Acad. Sci. U.S.A **68,** 1762-1766 (1971).
3. Akhmanova, A., Steinmetz, M.O.: Tracking the ends: a dynamic protein network controls the fate of microtubule tips. Nat. Rev. Mol. Cell Bio **9**, 309-322 (2008).
4. Nogales, E., Wang, H.-W.: Structural intermediates in microtubule assembly and disassembly: how and why? Curr. Opin. Cell Bio **18,** 179-184 (2006).
5. Calligaris, D., Verdier-Pinard, P., Devred, F., Villard, C., Braguer, D., Lafitte, D.: Microtubule targeting agents: from biophysics to proteomics. Cell. Mol. Life Sci **67,** 1089-1104 (2010).
6. Lewis, S. A., Wang, D., Cowan, N. J.: Microtubule-Associated Protein MAP2 Shares a Microtubule Binding Motif with Tau Protein. Sciences **11,** 936-939 (1988).
7. Sullivan, K. F., Cleveland, D. W.: Identification of conserved isotype-defining variable region sequences for four vertebrate beta tubulin polypeptide classes. Proc. Natl. Acad. Sci. U.S.A **83,** 4327-4331 (1986).
8. Ballestrem, C.; Magid, N.; Zonis, J.; Shtutman, M.; Bershadsky, A. In Interplay between the Actin Cytoskeleton, Focal Adhesions and Microtubules, Ridley, A.; Peckham, M.; Clark, P., Eds. Chichester, Wiley: 2004; pp 75-99.
9. Mane, J.Y., Semenchenko, V., Perez-Pineiro, R., Winter, P., Wishart, D., Tuszynski, J.A.: Experimental and Computational Study of the Interaction of Novel Colchicinoids with a Recombinant Human α I/β I-Tubulin Heterodimer. Chem. Bio. Drug Des **82,** 60-70 (2013).

10. Kline-Smith, S.L., Walczak, C.E.: Review: Mitotic Spindle Assembly and Chromosome Segregation. Refocusing on Microtubule Dynamics. Mol. Cell **15,** 317-327 (2004).

11. Wilson, L., Panda, D., Ann Jordan, M.: Modulation of Microtubule Dynamics by Drugs. A Paradigm for the Actions of Cellular Regulators. Cell Struct. Funct **24,** 329-335 (1999).

12. Schiff, P.B., Fant, J., Horwitz, S.B.: Promotion of microtubule assembly in vitro by taxol. Nature **277,** 665-667 (1979).

13. Bollag, D.M., McQueney, P.A., Zhu, J., Hensens, O., Koupal, L., Liesch, J., et al.: Epothilones, a new class of microtubule-stabilizing agents with a taxol-like mechanism of action. Cancer Res **55,** 2325-2333 (1995).

14. Canales, A., Rodriguez-Salarichs, J., Trigili, C., Nieto, L., Coderch, C., Andreu, J.M., et al.: Insights into the interaction of Discodermolide and Docetaxel with Tubulin. Mapping the Binding Sites of Microtubule-Stabilizing Agents by Using an Integrated NMR and Computational Approach. ACS Chem. Bio **6,** 789-799 (2011).

15. Wilmes, A., Bargh, K., Kelly, C., Northcote, P.T., Miller, J.H.: Peloruside a synergizes with other microtubule stabilizing agents in cultured cancer cell lines. Mol. Pharmaceutics **4,** 269-280 (2007).

16. Bhattacharyya, B., Panda, D., Gupta, S., Banerjee, M.: Anti-mitotic activity of colchicine and the structural basis for its interaction with tubulin. Med. Res. Rev **28,** 155-183 (2008).

17. Gigant, B., Wang, C., Ravelli, R.B.G., Roussi, F., Steinmetz, M.O., Curmi, P.A., et al.: Structural basis for the regulation of tubulin by vinblastine. Nature 519 (2005).

18. Bai, R., Pettit, G.R., Hamel, E.: Dolastatin 10, a powerful cytostatic peptide derived from a marine animal. Inhibition of tubulin polymerization mediated through the vinca alkaloid binding domain. Biochem. Pharmacol **39**, 1941-1949 (1990).

19. Anderson, H.J., Coleman, J.E., Andersen, R.J., Roberge, M.: Cytotoxic peptides hemiasterlin, hemiasterlin A and hemiasterlin B induce mitotic arrest and abnormal spindle formation. Cancer Chemoth. Pharm **39,** 223-226 (1997).

20. Jordan, M. A.; Wilson, L.: Microtubules as a target for anticancer drugs. Nat. Rev. Cancer **4,** 253-265 (2004).

21. Ravelli, R.B.G., Gigant, B., Curmi, P.A., Jourdain, I., Lachkar, S., Sobel, A., et al.: Insight into tubulin regulation from a complex with colchicine and a stathmin-like domain. Nature **428,** 198-202 (2004).

22. Schlesinger, N., Schumacher, R., Catton, M., Maxwell, L.: Colchicine for acute gout. Cochrane DB. Sys, 1-16 (2006).

23. Richette, P., Bardin, T.: Colchicine for the treatment of gout. Expert Opin. Pharmaco **11,** 2933-2938 (2010).

24. Dustin, P.: Microtubules. Berlin: New York : Springer-Verlag (1978)

25. Sun, L., Vasilevich, N.I., Fuselier, J.A., Coy, D.H.: Abilities of 3,4-diarylfuran-2-one analogs of combretastatin A-4 to inhibit both proliferation of tumor cell lines and growth of relevant tumors in nude mice. Anticancer Res **24,** 179-186 (2004).

26. Haar, E. T., Rosenkranz, H.S., Hamel, E., Day, B.W.: Computational and molecular modeling evaluation of the structural basis for tubulin polymerization inhibition by colchicine site agents. Bioorg. Med. Chem **4,** 1659-1671 (1996).

27. Fernando Díaz, J., Andreu, J.M.: Kinetics of dissociation of the tubulin-colchicine complex. Complete reaction scheme and comparison to thermodynamic measurements. J. Biol. Chem **266,** 2890-2896 (1991).

28. Menéndez, M., Laynez, J., Medrano, F.J., Andreu, J.M.: A thermodynamic study of the interaction of tubulin with colchicine site ligands. J. Biol. Chem **264,** 16367-16371 (1989).

29. Andreu, J.M., Gorbunoff, M.J., Medrano, F.J., Rossi, M., Timasheff, S.N.: Mechanism of colchicine binding to tubulin. Tolerance of substituents in ring C' of biphenyl analogues. Biochem **30,** 3777-3786 (1991).

30. Hastie, S.B.: Interactions of colchicine with tubulin. Pharmacol. Therapeut **51,** 377-401 (1991).

31. Banerjee, A., Luduena, R.F.: Kinetics of colchicine binding to purified beta-tubulin isotypes from bovine brain. J. Biol. Chem **267,** 13335-13339 (1992).

32. Tahir, S.K., Kovar, P., Rosenberg, S.H., Ng, S. C.: Rapid colchicine competition-binding scintillation proximity assay using biotin-labeled tubulin. Biotechniques **29,** 156-160 (2000).

33. Chabin, R.M., Hastie, S.B.: Association of thiocolchicine with tubulin. Biochem. Bioph. Res. Co **161,** 544-550 (1989).

34. Loo, J.A.: Studying noncovalent protein complexes by electrospray ionization mass spectrometry. Mass Spectrom. Rev **16,** 1-23 (1997).

35. Daniel, J.M., Friess, S.D., Rajagopalan, S., Wendt, S., Zenobi, R.: Quantitative determination of noncovalent binding interactions using soft ionization mass spectrometry. Int. J. Mass Spectrom **216,** 1 (2002).

36. Heck, A.J.R., Van Den Heuvel, R.H.H.: Investigation of intact protein complexes by mass spectrometry. Mass Spectrom. Rev **23,** 368-389 (2004).

37. Gabelica, V., Rosu, F., De Pauw, E.: A simple method to determine electrospray response factors of noncovalent complexes. Anal. Chem 6708 (2009).

38. Kitova, E.N., El-Hawiet, A., Schnier, P.D., Klassen, J.S.: Reliable Determinations of Protein-Ligand Interactions by Direct ESI-MS Measurements. Are We There Yet? J. Am. Soc. Mass Spectrom **23,** 431-441 (2012).

39. Wang, W. J., Kitova, E. N., Klassen, J. S.: Nonspecific Protein−Carbohydrate Complexes Produced by Nanoelectrospray Ionization. Factors Influencing Their Formation and Stability. Anal. Chem **77,** 3060-3071 (2005).

40. El-Hawiet, A., Shoemaker, G.K., Daneshfar, R., Kitova, E.N., Klassen, J.S.: Applications of a catch and release electrospray ionization mass spectrometry assay for carbohydrate library screening. Anal. Chem **84,** 50-58 (2012).

41. Han, L., Kitova, E., Tan, M., Jiang, X., Klassen, J.: Identifying Carbohydrate Ligands of a Norovirus P Particle using a Catch and Release Electrospray Ionization Mass Spectrometry Assay. J. Am. Soc. Mass Spectrom **25,** 111-119 (2014).

42. Leney, A. C.; Fan, X.; Kitova, E. N.; Klassen, J. S.: Nanodiscs and electrospray ionization mass spectrometry: a tool for screening glycolipids against proteins. Anal. Chem **86,** 5271-5277 (2014).

43. Cheng, X., Chen, R., Bruce, J.E., Schwartz, B.L., Anderson, G.A., Hofstadler, S.A., et al.: Using electrospray ionization FTICR mass spectrometry to study competitive binding of inhibitors to carbonic anhydrase. J. Am. Chem. Soc **117,** 8859-8860 (1995).

44. Gao, J., Cheng, X., Chen, R., Sigal, G.B., Bruce, J.E., Schwartz, B.L., et al.: Screening derivatized peptide libraries for tight binding inhibitors to carbonic anhydrase II by electrospray ionization-mass spectrometry. J. Med. Chem **39,** 1949-1955 (1996).

45. Han, L., Tan, M., Xia, M., Kitova, E. N., Jiang, X., Klassen, J. S.: Gangliosides are Ligands for Human Noroviruses. J. Am. Chem. Soc **136,** 12631-12637 (2014).

46. Zhang, Y., Liu, L., Daneshfar, R., Kitova, E.N., Caishun, L., Feng, J., et al.: Protein–Glycosphingolipid Interactions Revealed Using Catch-and- Release Mass Spectrometry. Anal. Chem **84,** 7618-7621 (2012).
47. El-Hawiet, A., Kitova, E.N., Klassen, J. S.: Quantifying Protein Interactions with Isomeric Carbohydrate Ligands Using a Catch and Release Electrospray Ionization-Mass Spectrometry Assay. Anal. Chem **85,** 7637-7644 (2013).
48. Luduena, R. F. Are tubulin isotypes functionally significant? Mol. Biol. Cell **4,** 445-457 (1993).
49. Redeker, V.; Melki, R.; Prome, D.; Le Caer, J-P.; Rossier, J.: Structure of tubulin C-terminal domain obtained by subtilisin treatment. The major alpha and beta tubulin isotypes from pig brain are glutamylated. FEBS. Lett. **313,** 185-192 (1992).
50. Leandro-García, L. J., Leskelä, S., Landa, I., Montero-Conde, C., López-Jiménez, E., Letón, R., et al.: Tumoral and tissue-specific expression of the major human β-tubulin isotypes. Cytoskeleton **67,** 214-223 (2010).
51. Torin Huzil, J., Ludueňa, R. F., Tuszynski, J. A.: Comparative modelling of human β tubulin isotypes and implications for drug binding. Nanotechnology **17,** S90-S100 (2006).
52. Ravanbakhsh, S., Gajewski, M., Greiner, R., Tuszynski, J. A.: Determination of the optimal tubulin isotype target as a method for the development of individualized cancer chemotherapy. Theor. Biol. Med. Model **10,** 1-18 (2013).

Figure captions

Figure 1. The structures of (a) colchicinoid drugs (**L1**- **L8**) and (b) vincristine (**L9**).

Figure 2. ESI mass spectra acquired in positive ion mode for (a) an aqueous ammonium acetate solution (100 mM, pH 6.8) of tubulin (14 μM), (b) an aqueous ammonium acetate solution (100 mM, pH 6.8) containing 0.05% DMSO (v/v) and tubulin (14 μM) alone and in the presence of **L1** at concentrations of (c) 2 μM, (d) 6 μM, (e) 14 μM and (f) 20 μM.

Figure 3. (a) ESI mass spectrum acquired in positive ion mode for an aqueous ammonium acetate solution (100 mM, pH 6.8) containing 0.05% DMSO (v/v) and tubulin (14 μM) with **L1** (14 μM) and **L9** (14 μM). CID mass spectra of tubulin ions, produced by ESI performed on the solution in (a) using Trap voltages of (b) 25 V, (c) 50 V, (d) 80 V, (e) 100 V and (f) 120 V.

Figure 4. (a) Plot of abundance ratio of **L1** to **L9** ions released by CID (in Trap) from tubulin ions, produced by ESI performed in positive ion mode on an aqueous ammonium acetate solution (100 mM, pH 6.8) containing 0.05% DMSO (v/v) and tubulin (14 μM) with **L1** (14 μM) and **L9** (14 μM), versus Trap voltage. (b) Abundance ratios of **L1** to **L9** ions (green bars) released by CID (in Trap) from tubulin ions, produced by ESI performed in positive ion mode on an aqueous ammonium acetate solution (100 mM, pH 6.8) containing 0.05% DMSO (v/v) and tubulin (14 μM) with **L1** and **L9** at equimolar concentrations (2 μM, 7 μM and 14 μM). The average value of the abundance ratio determined from these three concentrations is shown, as well as the expected value based on the reported affinities (Lit., shown in blue) [5, 32].

Figure 5. CID mass spectra of tubulin ions, produced by ESI performed in positive ion mode on an aqueous ammonium acetate solution (100 mM, pH 6.8) containing 0.05% DMSO (v/v) and tubulin (14 μM) with **L1 – L7** (2 μM each), at Trap voltages of (a) 2 V, (b) 25 V, (c) 50 V, (d) 80 V, (e) 100 V, (f) 120 V, (g) 140 V.

Figure 6. (a) Plot of abundance ratio of **L1 – L7** ions released by CID (in Trap) from tubulin ions, produced by ESI performed in positive ion mode on an aqueous ammonium acetate solution (100 mM, pH 6.8) containing 0.05% DMSO (v/v) and tubulin (14 μM) with **L1 – L7** (2 μM each). (b) Normalized (to **L3**) relative affinities of **L1 – L7** for tubulin measured by CaR-ESI-MS for an aqueous ammonium acetate solution (100 mM, pH 6.8) containing 0.05% DMSO (v/v) and tubulin (14 μM) with **L1 – L7** at (total) ligand concentrations of 2 μM (red bar), 7 μM (blue bar) and 14 μM (green bar). All measurements were carried out using a Trap voltage of 120 V.

a)

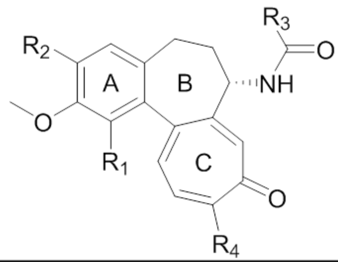

compound	MW	R1	R2	R3	R4
L1	399.2	$-OCH_3$	$-OCH_3$	$-CH_3$	$-OCH_3$
L2	415.1	$-OCH_3$	$-OCH_3$	$-CH_3$	$-SCH_3$
L3	445.2	$-OCH_3$	$-OCH_2CH_3$	$-OCH_3$	$-SCH_3$
L4	510.2	$-OCH_3$	$-OCH_3$	$-CH_2NHC(=O)CF_3$	$-OCH_3$
L5	526.1	$-OCH_3$	$-OCH_3$	$-CH_2NHC(=O)CF_3$	$-SCH_3$
L6	554.2	$-OCH_2CH_2OCH_3$	$-OCH_3$	$-CH_2NHC(=O)CF_3$	$-OCH_3$
L7	587.2	$-OCH_2$ *m*-Pyr	$-OCH_3$	$-CH_2NHC(=O)CF_3$	$-OCH_3$
L8	563.6	$-OCH_3$	$-OCH_6O_5$	$-CH_3$	$-SCH_3$

b)

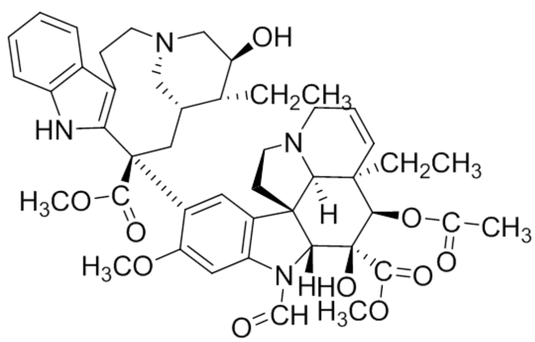

Figure 1

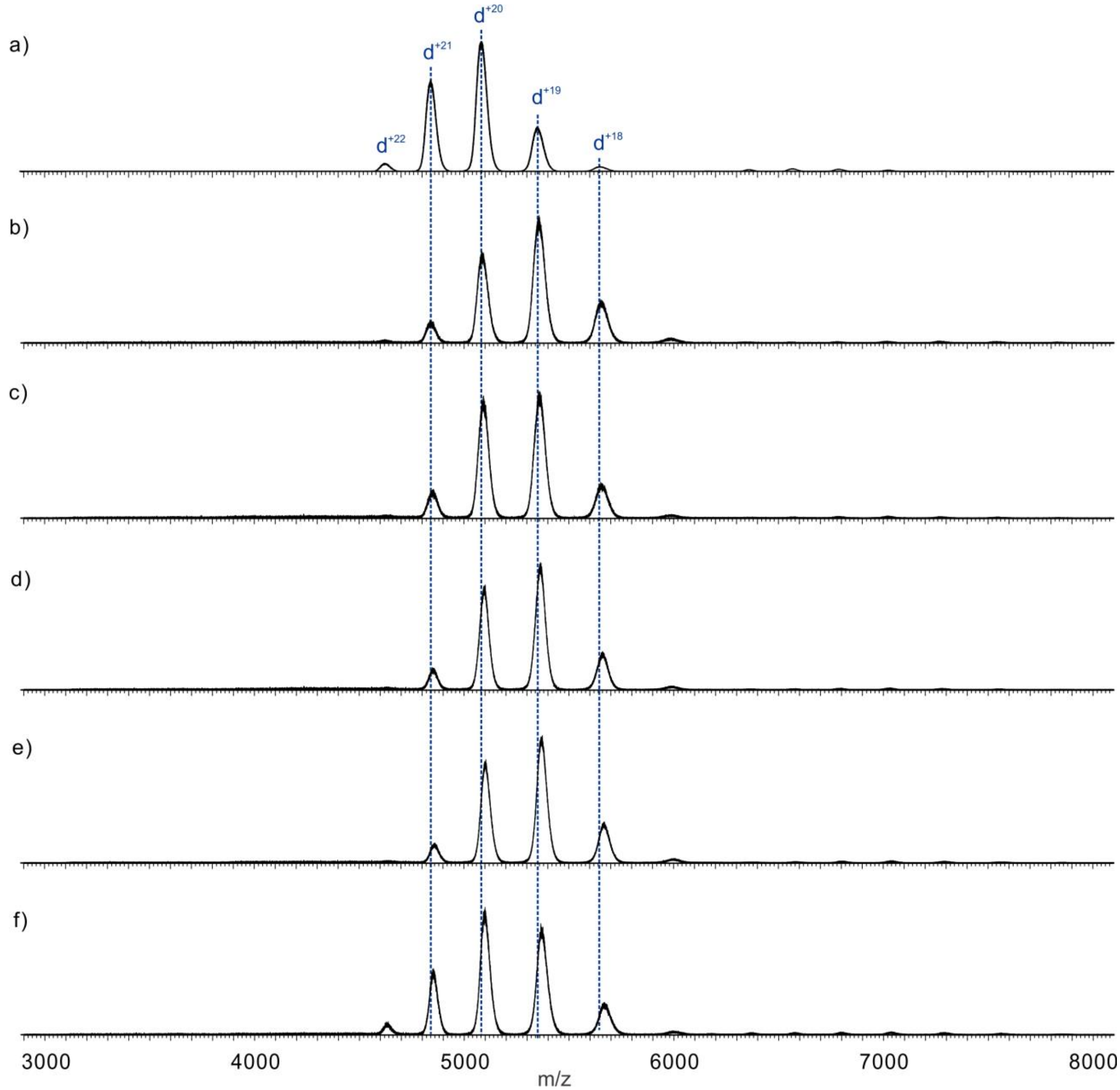

Figure 2

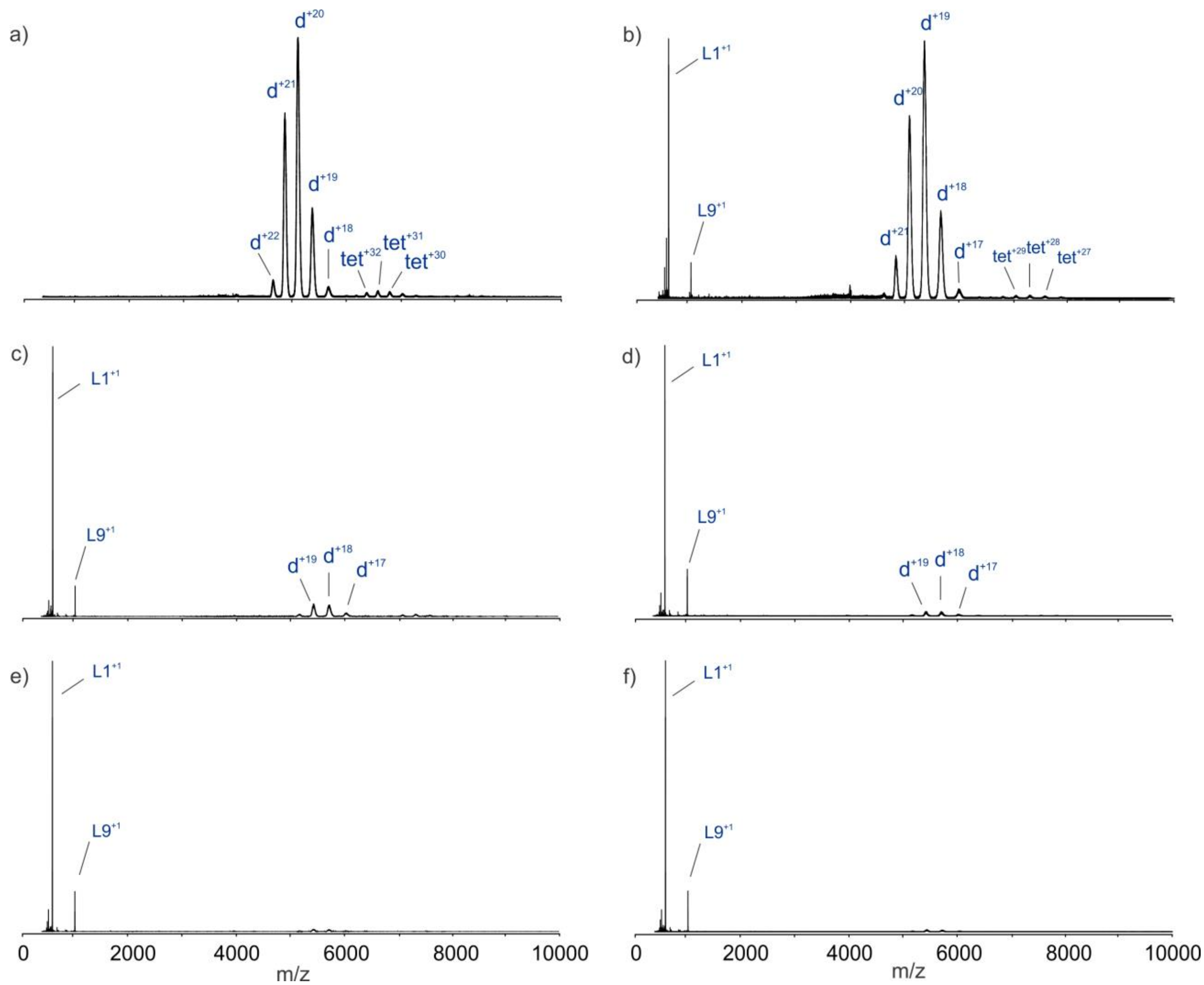

a)
d+20
d+21
d+19
d+22
d+18
tet+32
tet+31
tet+30
b)
L1+1
d+19
d+20
d+18
L9+1
d+21
d+17
tet+29
tet+28
tet+27
c)
L1+1
L9+1
d+19
d+18
d+17
d)
L1+1
L9+1
d+19
d+18
d+17
e)
L1+1
L9+1
f)
L1+1
L9+1
0
2000
4000
6000
8000
10000
m/z

Figure 3

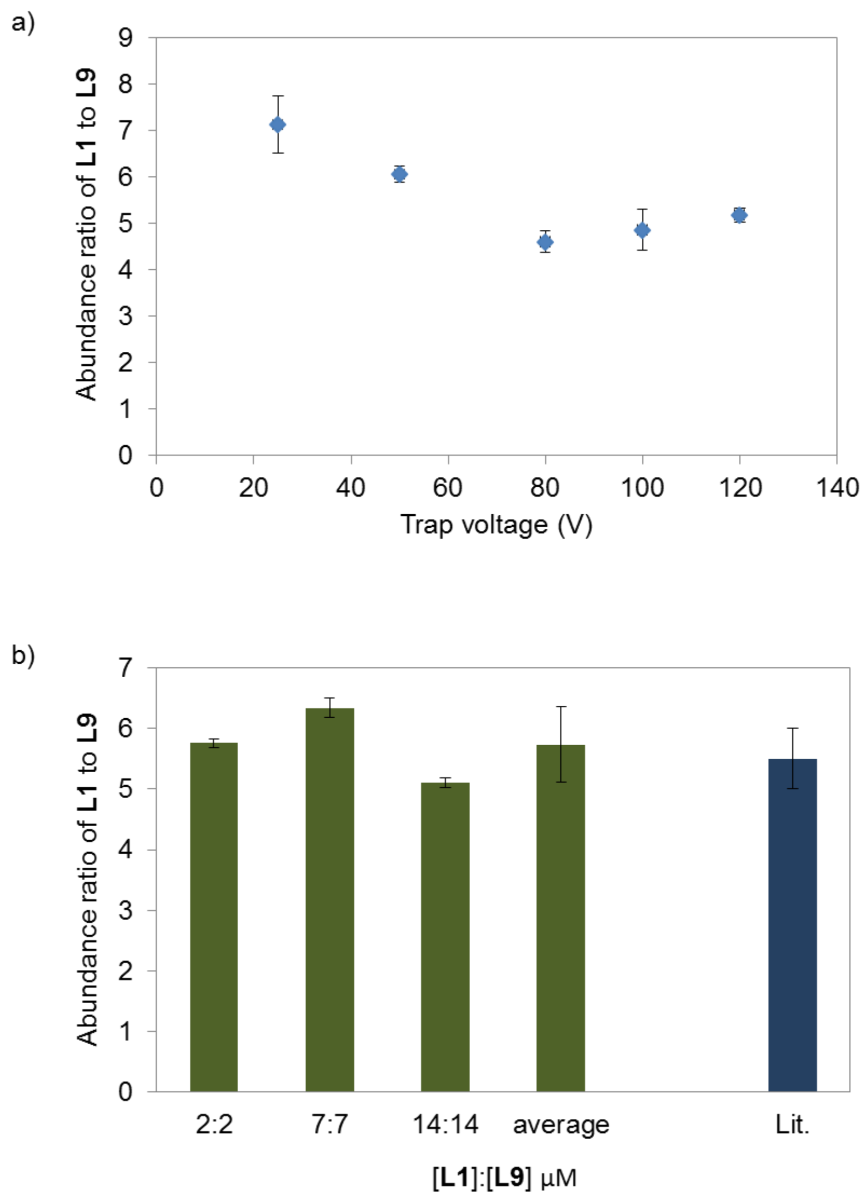
a)
Abundance ratio of L1 to L9
9
8
7
6
5
4
3
2
1
0
0
20
40
60
80
100
120
140
Trap voltage (V)
b)
Abundance ratio of L1 to L9
7
6
5
4
3
2
1
0
2:2
7:7
14:14
average
Lit.
[L1]:[L9] µM

Figure 4

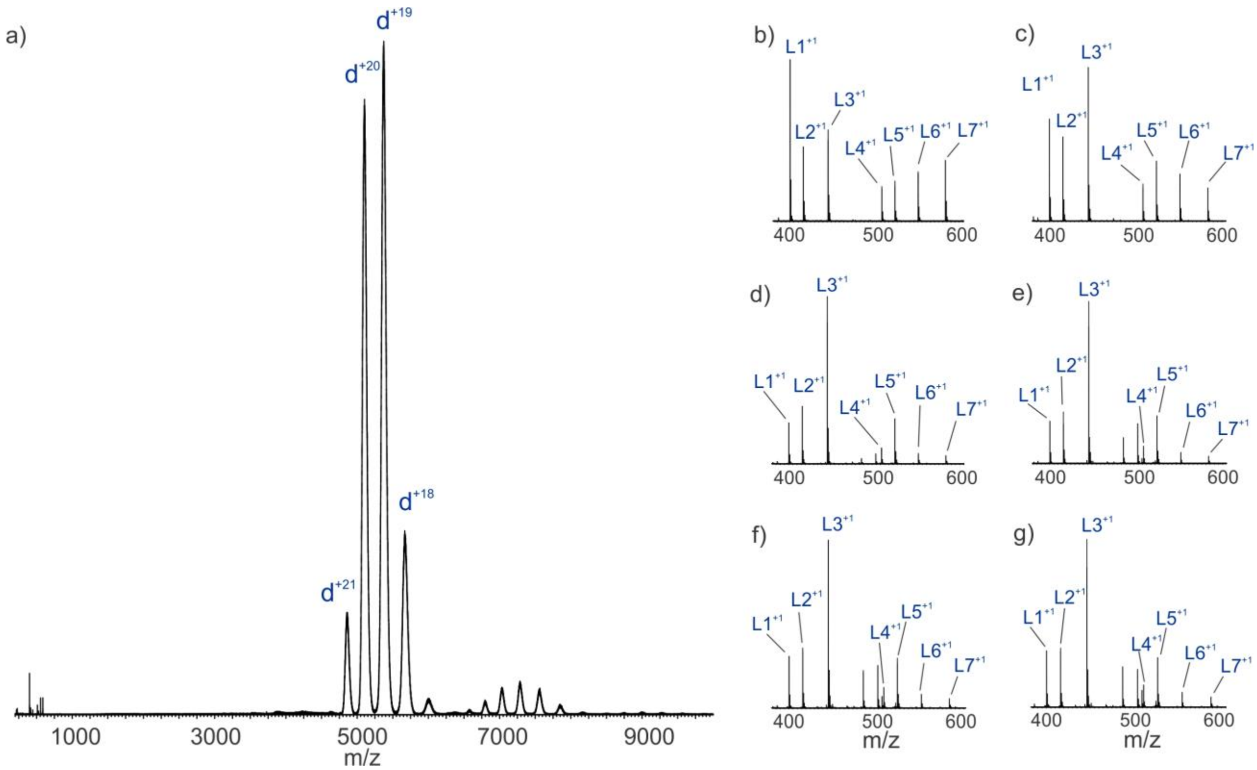
a)
d+19
d+20
d+18
d+21
1000
3000
5000
7000
9000
m/z
b)
c)
d)
e)
f)
g)
L1+1
L2+1
L3+1
L4+1
L5+1
L6+1
L7+1
400
500
600
m/z

Figure 5

a)

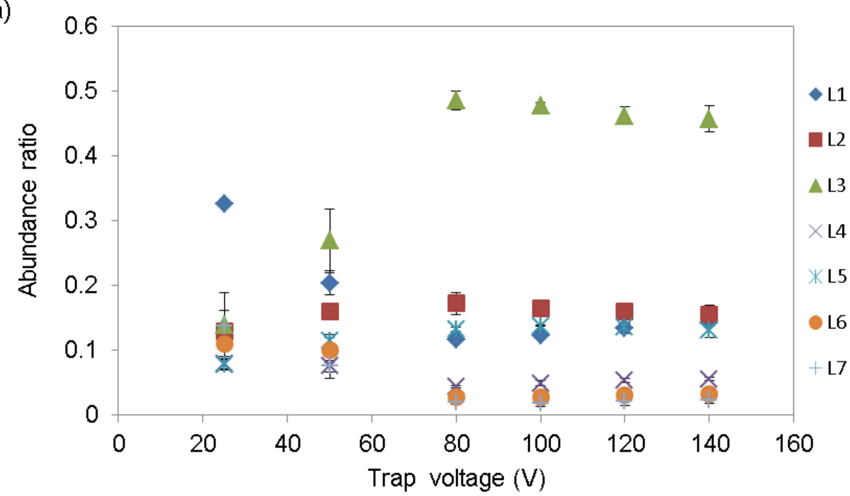
Abundance ratio
0.6
0.5
0.4
0.3
0.2
0.1
0
0
20
40
60
80
100
120
140
160
Trap voltage (V)
L1
L2
L3
L4
L5
L6
L7

b)

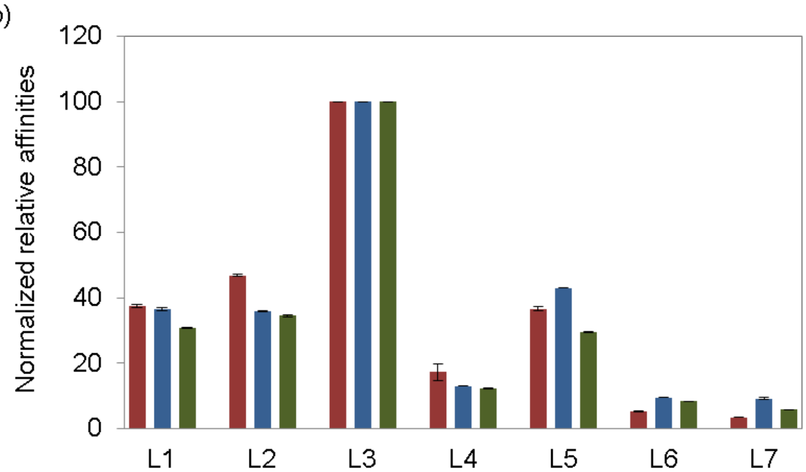
Normalized relative affinities
120
100
80
60
40
20
0
L1
L2
L3
L4
L5
L6
L7

Figure 6

Supplementary Information for:
Screening Anti-Cancer Drugs against Tubulin using Catch-and-Release Electrospray Ionization Mass Spectrometry

Reza Rezaei Darestani, Philip Winter, Elena N. Kitova, Jack A. Tuszynski, John S. Klassen

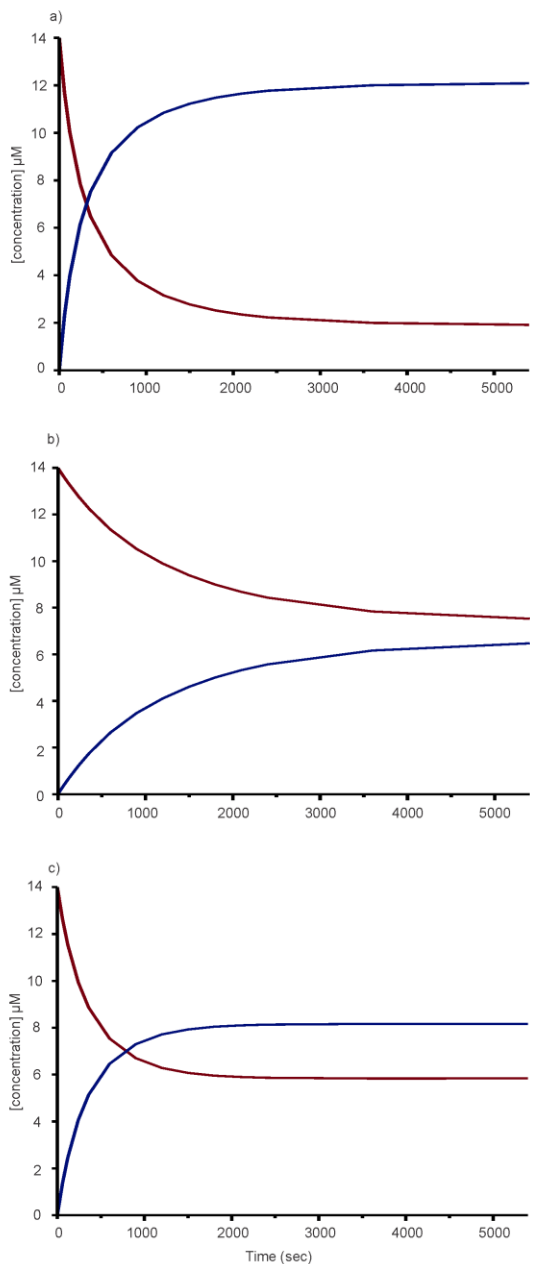

Figure S1. Calculated equilibration times for colchicine (14 µM) binding to different tubulin (14 µM) isotypes (a) αβII (k_2 of 132 ± 5 M^{-1} s^{-1}), (b) αβIII (k_2 of 30 ± 2 M^{-1} s^{-1}), and (c) αβIV (k_2 of 236 ± 5 M^{-1} s^{-1}) at 37 °C. The blue and red lines show the change in concentration of the product (tubulin-colchicine complex) and reactants (tubulin and colchicine), respectively.

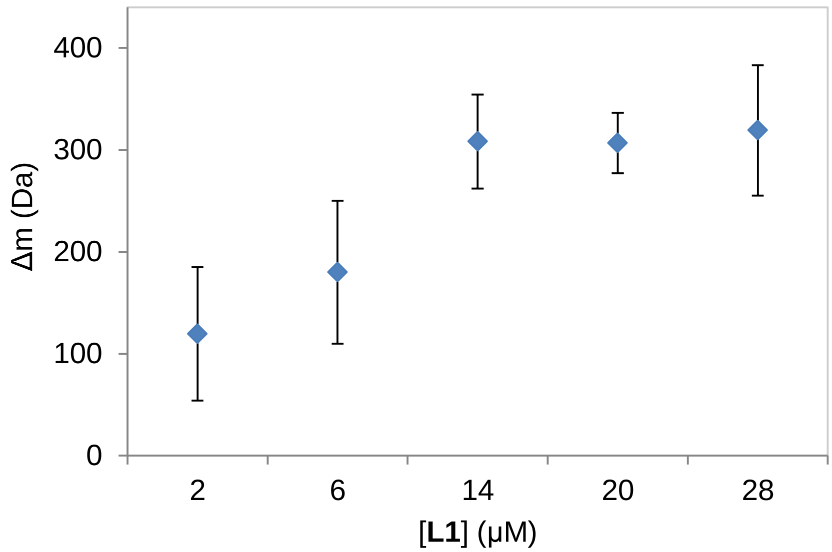

Figure S2. Change in the apparent molecular weight (Δm) of the tubulin dimer (based on the tubulin dimer ions d^{+17}– d^{+21}) measured by ESI-MS for aqueous ammonium acetate solutions (100 mM, pH 6.8) containing 0.05% DMSO (v/v), tubulin (14 μM) and colchicine (**L1**) at concentrations ranging from 2 to 28 μM.

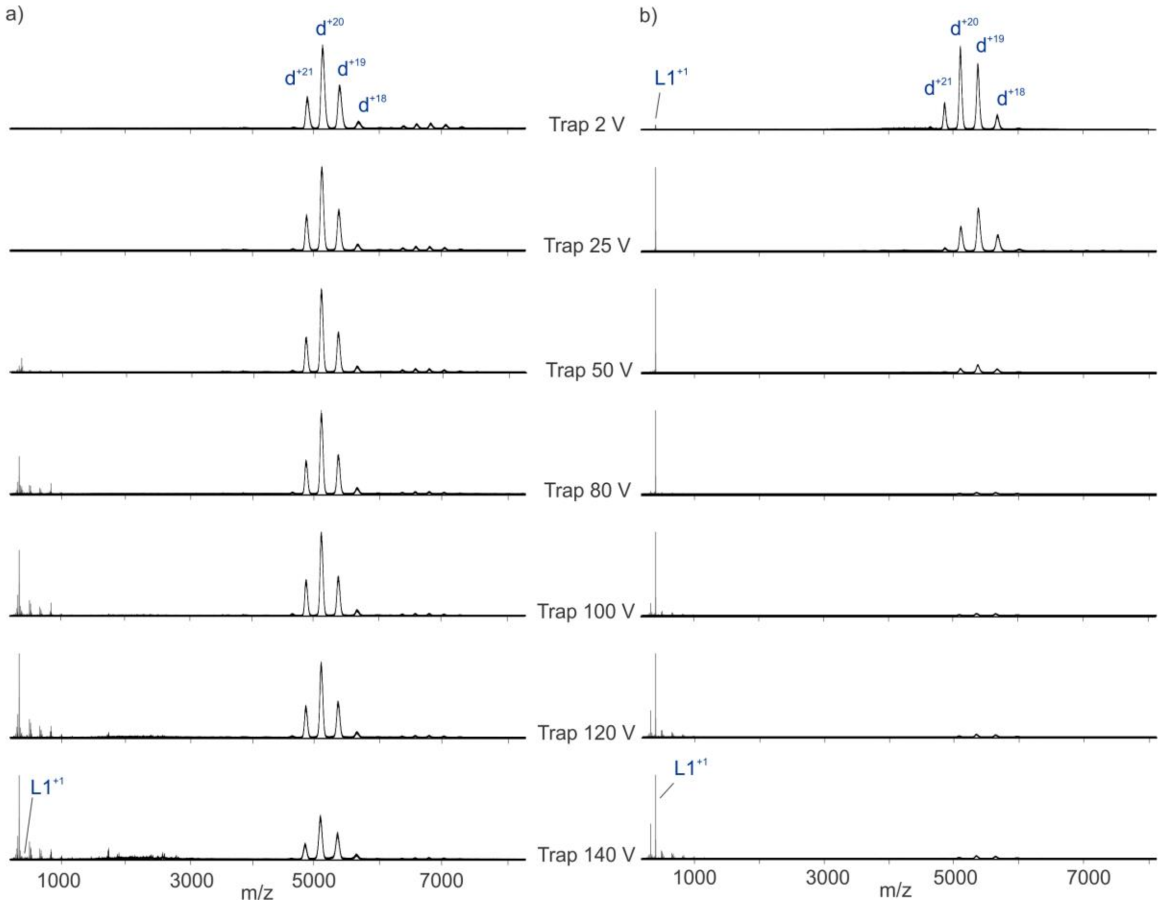

Figure S3. CID mass spectra of tubulin ions, produced by ESI performed in positive ion mode on an aqueous ammonium acetate solution (100 mM, pH 6.8) containing 0.05% DMSO (v/v) and (a) tubulin (14 μM) and (b) tubulin (14 μM) with **L1** (14 μM), using Trap voltages of 2 V, 25 V, 50 V, 80 V, 100 V, 120 V, and 140 V.

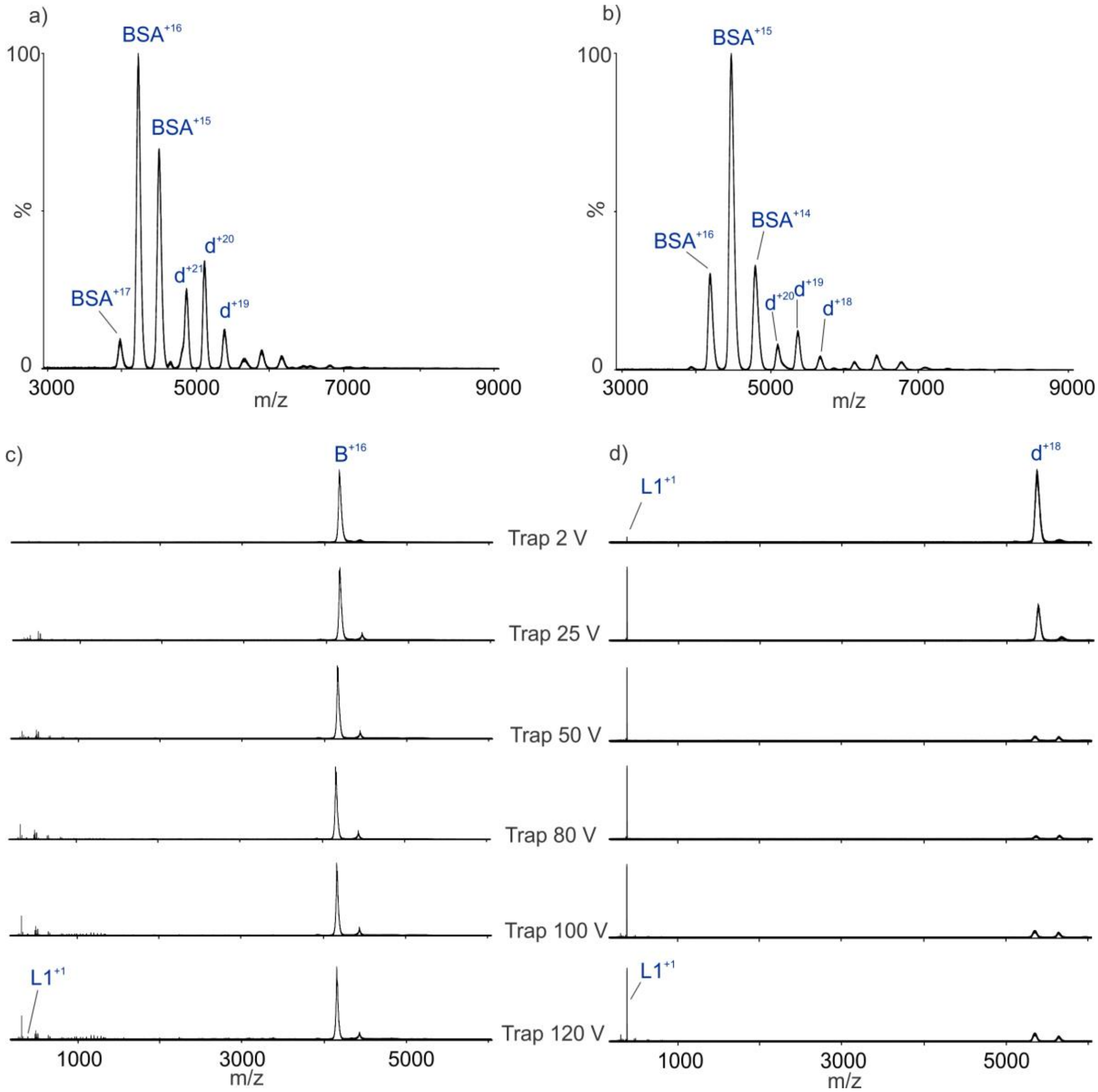

Figure S4. ESI mass spectra acquired in positive ion mode for aqueous ammonium acetate solutions (100 mM, pH 6.8) containing 0.05% DMSO (v/v) and (a) tubulin (14 μM) and BSA (14 μM) and (b) tubulin (14 μM), BSA (14 μM) and **L1** (14 μM) in ammonium acetate buffer (100 mM) at 37 °C for 1h. CID mass spectra of (c) +16 charge state of BSA (B^{+16}) and (d) tubulin +18 charge state of tubulin (d^{+18}), produced by ESI performed in positive ion mode on an aqueous ammonium acetate solution (100 mM, pH 6.8) of tubulin (14 μM), BSA (14 μM) and colchicine (**L1**, 14 μM), at Trap voltages ranging from 2 V to 120 V.

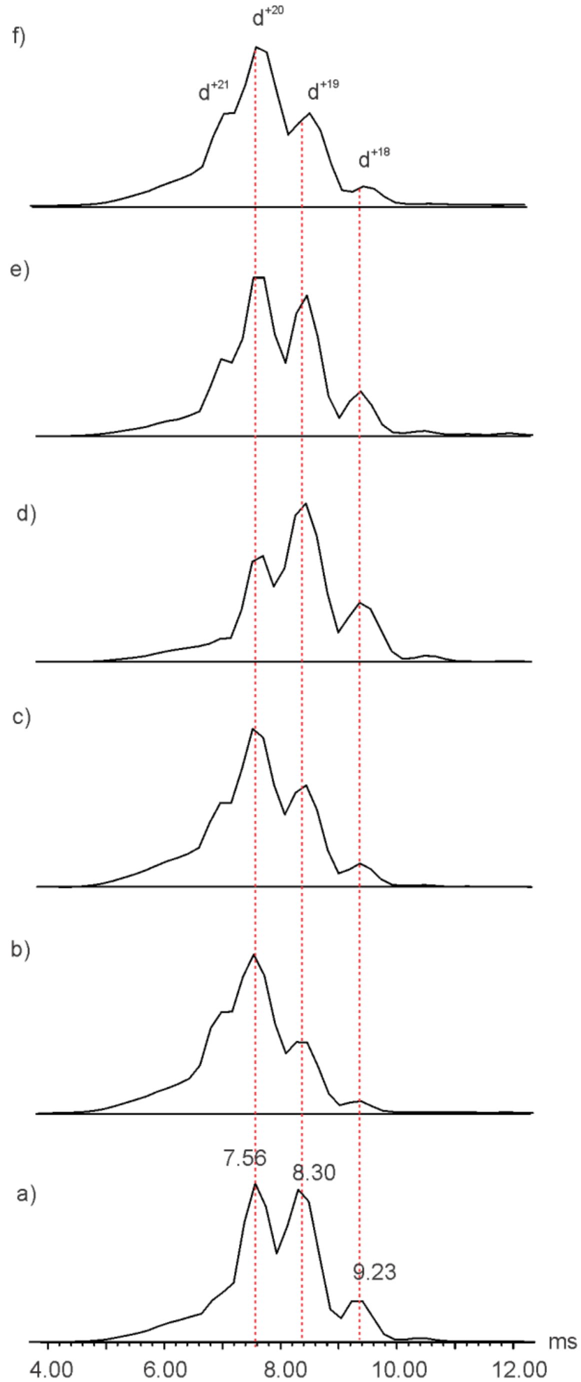

Figure S5. Arrival time distributions (ATDs) acquired in positive ion mode for an aqueous ammonium acetate solutions (100 mM, pH 6.8) containing 0.05% DMSO (v/v) and tubulin (14 μM) alone and with colchicine (**L1**) at concentrations of (b) 2 μM, (c) 6 μM, (d) 14 μM, (e) 20 μM, and (f) 28 μM.

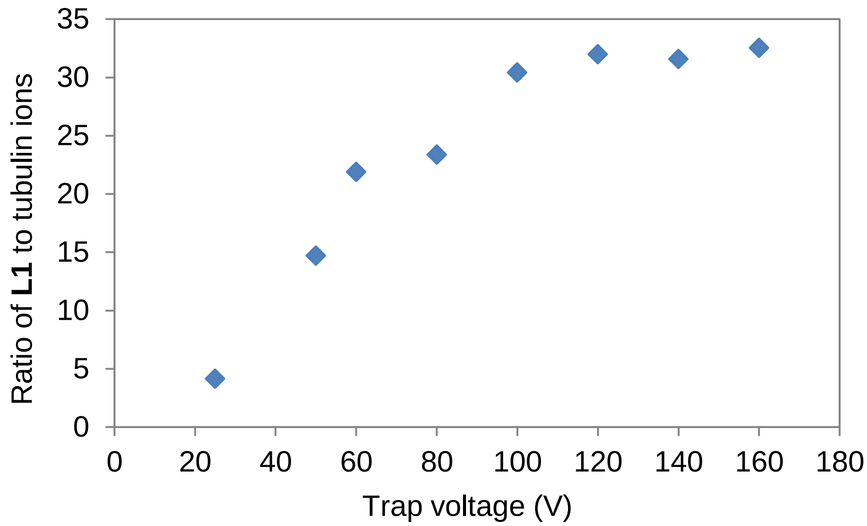

Figure S6. Abundance ratio of **L1** ions, released by CID (in Trap) from tubulin ions, produced by ESI performed in positive ion mode on an aqueous ammonium acetate solution (100 mM, pH 6.8) containing 0.05% DMSO (v/v) and tubulin (14 µM) with **L1** (14 µM), to the tubulin d^{+18}–d^{+21} ions measured as a function of Trap voltage.

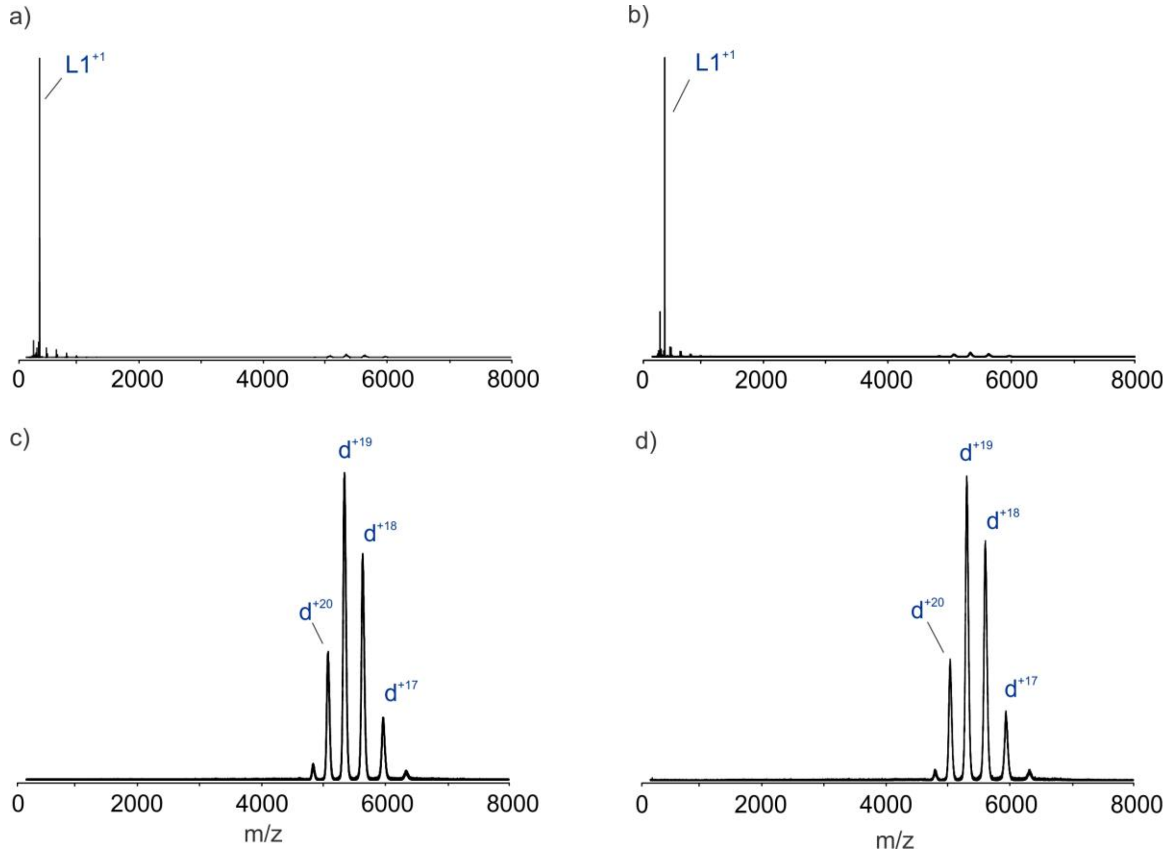

Figure S7. CID mass spectra of tubulin ions, produced by ESI performed in positive ion mode on an aqueous ammonium acetate solution (100 mM, pH 6.8) of tubulin (14 μM) and colchicine (**L1**, 14 μM), at Trap and Transfer voltages of (a) Trap 100 V/Transfer 1 V, (b) Trap 1 V/Transfer 100 V, (c) Trap 100 V/Transfer 1V, (d) Trap 100 V/Trans 100 V. In (c) and (d), any **L1** ions produced in the Trap region were excluded from the CID spectra based on IMS arrival times.

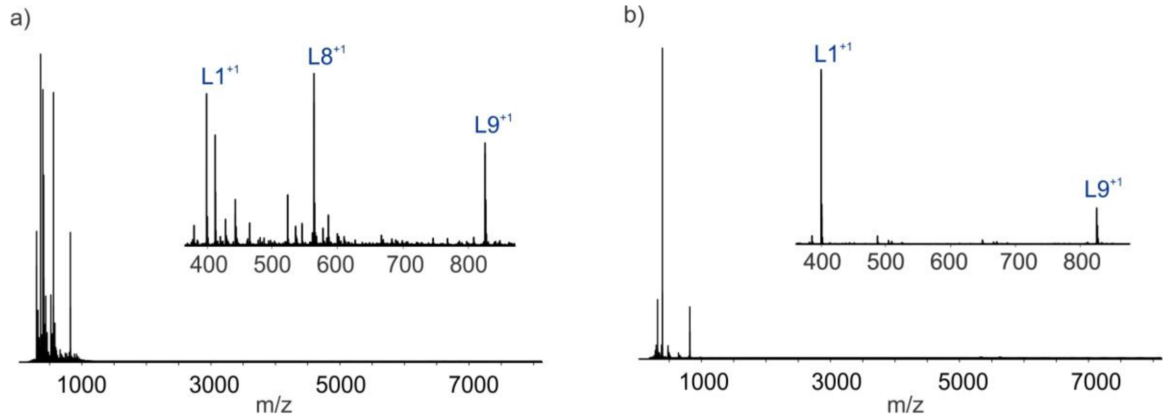

Figure S8. (a) ESI mass spectrum acquired in positive ion mode for an aqueous ammonium acetate solution (100 mM, pH 6.8) containing 0.05% DMSO (v/v) and equimolar concentrations (14 μM) of tubulin, **L1**, **L8**, and **L9**. (b) CID mass spectrum of tubulin ions, produced by ESI performed in positive ion mode on the solution described in (a), using a Trap voltage of 120 V.